Dalton
Transactions

ROYAL SOCIETY
OF CHEMISTRY

PAPER

View Article Online
View Journal

Check for updates

Cite this: DOI: 10.1039/d0dt03688a

Forays into rhodium macrocyclic chemistry stabilized by a P_2N_2 donor set. Activation of dihydrogen and benzene†

Alyssa Yeo, Corey A. Sanz and Michael D. Fryzuk *

The reaction of the dilithium diamido–diphosphine macrocycle, $Li_2[N(SiMe_2CH_2P(Ph)CH_2SiMe_2)_2N]$ ($Li_2[P_2N_2]$) with $[Rh(COD)Cl]_2$ generates the dirhodium macrocyclic compound, $[P_2N_2][Rh(COD)]_2$ (where COD = η^4-1,5-cyclooctadiene), wherein both rhodium-COD units are *syn* to each other and have square planar geometries. While this dirhodium derivative does react with H_2, no clean products could be isolated. Upon reaction of $Li_2[P_2N_2]$ with $[Rh(COE)_2Cl]_2$ (where COE is η^2-cyclooctene), the dilithium–dihodium derivative $([Rh(COE)][P_2N_2]Li)_2$(dioxane) forms, which was characterized by single-crystal X-ray analysis and NMR spectroscopy. The cyclooctene derivative reacts with dihydrogen in benzene to generate the dilithium–dirhodium-dihydride complex $([Rh(H)_2][P_2N_2]Li)_2$(dioxane); also formed is the dilithium–dirhodium–phenylhydride complex $([Rh(C_6H_5)H][P_2N_2]Li)_2$(dioxane) *via* oxidative addition of a C–H bond of the solvent. The phenyl-hydride is eventually converted to the dihydride derivative *via* further reaction with H_2. This process is complicated by adventitious H_2O, which leads to the isolation of the amine-dihydride, $Rh[P_2N_2H](H)_2$; drying of the H_2 eliminates this side product. Nevertheless, careful addition of H_2O to $([Rh(COE)][P_2N_2]Li)_2$(dioxane) results in protonation of one of the amido units and the formation of the rhodium–amine cyclooctene derivative, $Rh[P_2N_2H]$(COE), which upon reaction with H_2 generates the aforementioned amine-dihydride, $Rh[P_2N_2H](H)_2$. The mechanism by which dihydrogen and C–H bonds of benzene are activated likely involves initial dissociation of cyclooctene from the 18-electron centers in $([Rh(COE)][P_2N_2]Li)_2$(dioxane), followed by H–H and C–H bond activation. The ability of one of the amido units of the P_2N_2 macrocycle to be protonated is a potentially useful proton storage mechanism and is of interest in other bond activation processes.

Received 25th October 2020,
Accepted 2nd December 2020

DOI: 10.1039/d0dt03688a

rsc.li/dalton

Introduction

The organometallic chemistry of rhodium is dominated by the study of Rh complexes that have relevance to catalytic processes.[1] A large number of pincer complexes of rhodium have been developed, containing a variety of mixed-donor ligand arrays.[2] Several rhodium pincer complexes have proven useful in catalytic transformations, such as dimerization of terminal alkynes,[3] alkane transfer-dehydrogenation,[4] metal–ligand cooperativity,[5] and functionalization of C–H bonds.[6]

A recurring characteristic amongst the aforementioned rhodium derivatives is the use of P and/or N-containing ligands. The synthesis of a number of rhodium complexes employing phosphorus- and/or nitrogen-containing ligand arrangements has previously been reported by our group,[7] in particular, early work focused on amidodiphosphine complexes of rhodium utilizing the [PNP] ligand framework (where [PNP] = $[N(SiMe_2CH_2PPh_2)_2]$).[8] Other related PNP donor sets have been prepared and their rich chemistry explored.[3,5,6,9] The synthesis of the [PNP] rhodium cyclooctene (COE) complex and subsequent reactivity with H_2 [8c] are shown in Scheme 1. Although numerous transition metal complexes of our [PNP] and related macrocyclic $[P_2N_2]$ ligand sets are known,[10] the synthesis of rhodium complexes of $[P_2N_2]$ was not previously explored.

Macrocyclic complexes of rhodium are known and typically involve rigid, planar arrays of N-donors as in porphryins and tetraazaannulene derivatives.[11] For example, Rh(TMP) (where TMP = tetramesitylporphyrin) and Rh(TMTAA) (where TMTAA = dibenzotetranethylazaannulene) display remarkable behavior that includes C–H activation, Rh–H addition to CO, alkenes, and activation of H_2O.

University of British Columbia, Department of Chemistry, Vancouver, BC, Canada. E-mail: fryzuk@chem.ubc.ca

† Electronic supplementary information (ESI) available: Additional experimental details, copies of NMR spectra for all new complexes, X-ray data collection and refinement procedures. CCDC 2004254, 2004255, 2005434–2005436 and 2024716. For ESI and crystallographic data in CIF or other electronic format see DOI: 10.1039/d0dt03688a

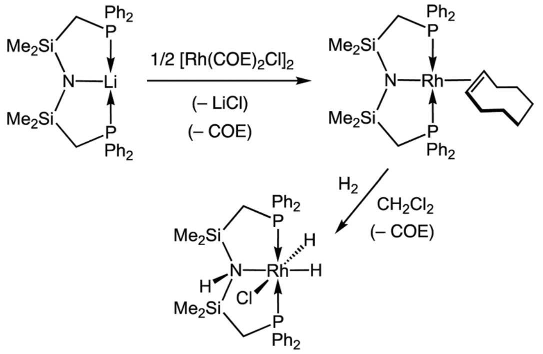

Scheme 1 Synthesis of the Rh[PNP](COE) complex and its reaction with H_2 in CH_2Cl_2.

In this report, the synthesis and reactivity of macrocyclic $[P_2N_2]$ rhodium complexes are investigated with particular interest in exploring the ability of these systems to undergo oxidative addition of H_2. Such studies could set the stage to utilizing these macrocyclic rhodium derivatives in catalytic processes.

Results and discussion

Synthesis and reactivity of $[P_2N_2][Rh(COD)]_2$

Initial exploration into coordinating $[P_2N_2]$ to rhodium began by treatment of *syn*-$Li_2[P_2N_2]$ with half an equivalent of the readily available Rh(I) starting material, $[Rh(COD)Cl]_2$, anticipating the formation of a square-planar, anionic Rh(I) species such as $Li[P_2N_2]Rh$, by release of 1,5-cyclooctadiene. Surprisingly, upon examination of the $^{31}P\{^1H\}$ NMR spectrum of the reaction mixture, peaks corresponding to unreacted *syn*-$Li_2[P_2N_2]$ were observed along with a doublet at δ 20.0 indicating a new Rh-containing complex was generated. The Rh–P coupling (143 Hz) observed in the $^{31}P\{^1H\}$ NMR spectrum is indicative of a Rh(I) species.[12] The ^1H NMR spectrum of the material isolated from the reaction also revealed resonances suggestive of two coordinated COD molecules (*via* integration relative to the silyl-methyl protons). As a result, it was proposed that the new species contains two rhodium COD units per $[P_2N_2]$ ligand. Treatment of *syn*-$Li_2[P_2N_2]$ with one equivalent of dimer $[Rh(COD)Cl]_2$ afforded yellow crystalline material, giving rise to the same resonances observed in the previous NMR spectra, absent of unreacted *syn*-$Li_2[P_2N_2]$. Scheme 2 shows the formation of this new rhodium species as $[P_2N_2][Rh(COD)]_2$ (**1**).

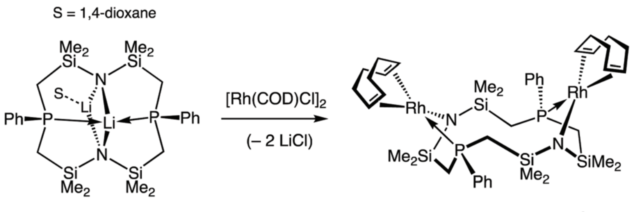

syn-$Li_2[P_2N_2]$ $[P_2N_2][Rh(COD)]_2$ **1**

Scheme 2 Reaction of *syn*-$Li_2[P_2N_2]$ with $[Rh(COD)Cl]_2$ to generate $[P_2N_2][Rh(COD)]_2$ (**1**).

Single crystals of **1** were isolated and subjected to X-ray diffraction studies. The solid-state molecular structure of this dirhodium species is shown in Fig. 1 with selected bond lengths and angles. Both rhodium atoms are coordinated on the same side of the $[P_2N_2]$ macrocycle. Each Rh(I) center is coordinated to one amido and one phosphine donor on $[P_2N_2]$, as well as one COD molecule, generating a distorted square planar geometry, thus generating essentially identical environments around each rhodium. The Rh–P and Rh–N bond distances (2.3082(10), 2.2834(10) Å and 2.163(3), 2.143(3) Å respectively) in $[P_2N_2][Rh(COD)]_2$ (**1**) are consistent with those reported for rhodium COD complexes coordinated to P,N-donor ligands.[13] The Rh–COD bond distances differ with respect to the C═C moiety coordinating in either a *cis* or *trans* position relative to the phosphine. The Rh–COD(*trans*) bond distances of 2.108 and 2.101 Å are longer than the Rh–COD(*cis*) bond distances of 2.005 and 1.984 Å. In addition, the C–C bond lengths of the *trans* C═C moieties (1.373(6) and 1.361(6) Å) are slightly shorter than the bond lengths of the *cis* C═C moieties (1.398(6) and 1.405(5) Å). This difference in bond distances suggests that the *trans* disposed C═C moieties are less activated and less strongly bound to the rhodium centres, as a result of the *trans* influence from the phosphines.[7d] One further point is the fact that the P_2N_2 framework is quite flexible as evident from the conformation of the 12-membered heteroatom ring that supports the two Rh(COD) units in local square-planar environments.

In an effort to drive the reaction of *syn*-$Li_2[P_2N_2]$ with $[Rh(COD)Cl]_2$ towards formation of a complex with only one rhodium coordinated to $[P_2N_2]$ (potentially $Li[P_2N_2]Rh$ *via* displacement of COD), a THF solution of *syn*-$Li_2[P_2N_2]$ with 0.5 equivalents of $[Rh(COD)Cl]_2$ was heated at 60 °C for 12 h. In the $^{31}P\{^1H\}$ NMR spectrum of the reaction mixture, three new doublet resonances at δ 13.2, 22.8 and 32.8 (with Rh–P coupling constants of 202, 127, and 108 Hz, respectively) were

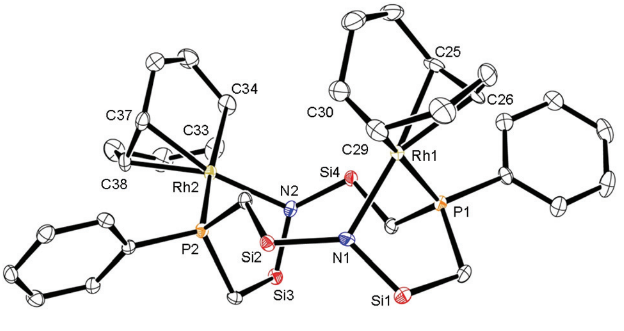

Fig. 1 ORTEP depiction (ellipsoids at 50% probability) of $[P_2N_2][Rh(COD)]_2$ (**1**). Silyl methyl carbons and all hydrogen atoms are omitted for clarity. Selected bond lengths (Å) and angles (°): Rh1–N1, 2.163(3); Rh1–P1, 2.3082(10); C29–C30 (*trans* to P1), 1.373(6); C25–C26 (*cis* to P1), 1.398(6); Rh1–COD(*trans* to P1)$_{cent}$, 2.108; Rh1–COD(*cis* to P1)$_{cent}$, 2.005; Rh2–N2, 2.143(3); Rh2–P2, 2.2834(10); C33–C34 (*trans* to P2), 1.361(6); C37–C38 (*cis* to P2), 1.405(5); Rh2–COD(*trans* to P2)$_{cent}$, 2.101; Rh2–COD(*cis* to P2)$_{cent}$, 1.984; N1–Rh1–P1, 82.07(9); N2–Rh2–P2, 82.37(9).

observed, in addition to the doublet at δ 20.0 for the aforementioned complex $[P_2N_2][Rh(COD)]_2$. Attempts to isolate or separate these species were unsuccessful. Postulating that these new species could arise from thermal rearrangement of **1**, its thermal stability was also explored. After heating a solution of **1** at 60 °C for 12 h, there was no change observed in the $^{31}P\{^1H\}$ NMR and ^1H NMR spectra, indicating that it is not prone to thermal rearrangement or decomposition under these conditions. Accordingly, the addition of heat in the treatment of *syn*-$Li_2[P_2N_2]$ with $[Rh(COD)Cl]_2$ gave rise to new rhodium complexes independently of $[P_2N_2][Rh(COD)]_2$.

Reactivity of $[P_2N_2][Rh(COD)]_2$ with H_2

In the interest of activating H_2 and generating a rhodium hydride species, treatment of the dirhodium-COD derivative with H_2 was explored. Exposure of a toluene solution of **1** to 4 atm of H_2 resulted in the appearance of new resonances in the $^{31}P\{^1H\}$ NMR spectrum of the reaction mixture. However, after stirring under 4 atm of H_2 at RT for 3 days, the starting dirhodium complex was still present in a significant amount. Interestingly, upon heating the reaction mixture at 80 °C, both in the presence and absence of H_2, the remaining $[P_2N_2][Rh(COD)]_2$ complex was consumed. Unfortunately, the reaction does not proceed cleanly and a mixture of products is observed *via* NMR spectroscopy. The major species present displays a doublet resonance at δ 33.6 in the $^{31}P\{^1H\}$ NMR spectrum, with a Rh–P coupling of 96 Hz suggestive of a Rh(III) species. In the ^1H NMR spectrum, resonances corresponding to the coordinated COD in **1** have disappeared and new resonances at δ −14 and −18 have appeared, suggesting the presence of rhodium hydrides. Attempts to isolate species for further NMR spectroscopy and X-ray crystallography studies were unsuccessful and thus the nature of the products remains unknown.

Synthesis and reactivity of $([Rh(COE)][P_2N_2]Li)_2(dioxane)$

As outlined above, preliminary oxidative addition experiments of H_2 with the $[P_2N_2][Rh(COD)]_2$ system proved challenging, perhaps due to the difficulty in displacing the strongly-coordinated COD unit. In the interest of synthesizing a $[P_2N_2]$ rhodium species with a more labile unit than COD, coordination of $[P_2N_2]$ to rhodium using $[Rh(COE)_2Cl]_2$ was investigated, the idea being that cyclooctene (COE) would be monodentate as opposed to the bidentate 1,5-cyclooctadiene (COD). Treatment of *syn*-$Li_2[P_2N_2]$ with $[Rh(COE)_2Cl]_2$ afforded a yellow solid, giving rise to two new doublet of doublets at δ 11.5 and δ 23.1 in the $^{31}P\{^1H\}$NMR spectrum. The phosphines are inequivalent, coupling to each other (J_{PP} = 384 Hz), and coupling to rhodium (J_{RhP} = 123 Hz and 114 Hz, suggestive of a Rh(I) species). In the $^1H\{^{31}P\}$ NMR spectrum, a strong singlet was observed at δ 3.6, suggestive of the presence of a coordinated dioxane molecule. X-ray diffraction studies confirmed the structure of a single complex that matches the NMR spectroscopy data. Scheme 3 shows the formation of the new dirhodium–dilithium complex, $([Rh(COE)][P_2N_2]Li)_2$-(dioxane) (**2**).

The solid-state molecular structure of **2** is shown in Fig. 2. This complex contains two $[P_2N_2]$ rhodium–lithium units

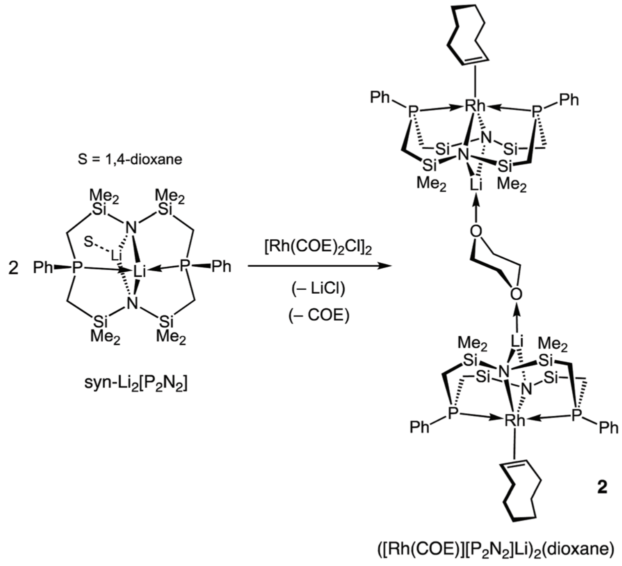

Scheme 3 Synthesis of the dirhodium–dilithium complex **2**.

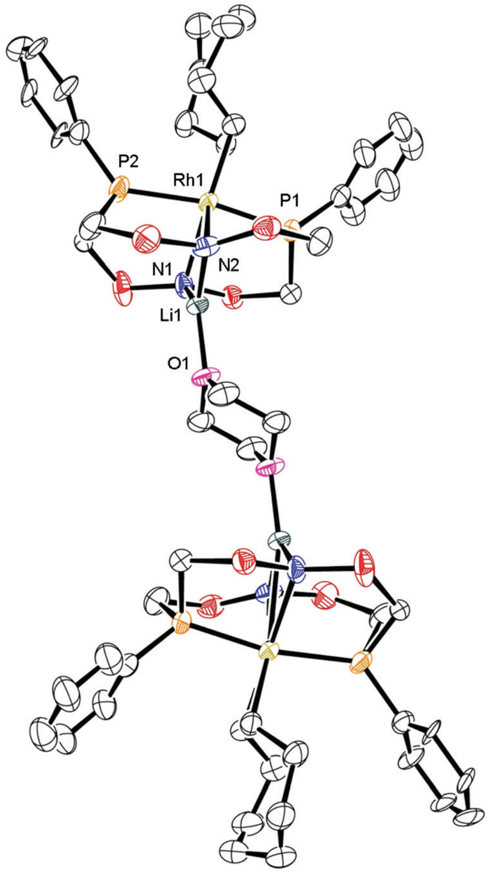

Fig. 2 ORTEP depiction (ellipsoids at 50% probability) of $([Rh(COE)][P_2N_2]Li)_2(dioxane)$ (**2**). Silyl methyl carbons and all hydrogen atoms are omitted for clarity. Selected bond lengths (Å) and angles (°): Rh1–N1, 2.453(4); Rh1–N2, 2.453(4); Rh1–P1, 2.2996(11); Rh1–P2, 2.344(8); N1–Li1, 1.951(7); N2–Li1, 1.971(8); P1–Rh1–P2, 166.10(17); N1–Rh1–N2, 85.94(11); N1–Li1–N2, 116.1(4).

bridged by a Li-coordinated dioxane molecule. The geometry about each Rh(I) centre is distorted trigonal bipyramidal, with one COE coordinated to each rhodium; the lithium ion bridges the two disilylamido units of the macrocycle. The inequivalent phosphines are generated by the η^2-COE unit binding mode and lack of rotation on the NMR time scale. Attempts to equilibrate the phosphorus-31 environments by heating in non-aromatic solvents (*vide infra*) led to some broadening but also new products were formed that were not pursued.

Reactivity of ([Rh(COE)][P_2N_2]Li)$_2$(dioxane) with H_2

Given our earlier success with oxidative addition of H_2 to the square planar Rh(COE)[PNP] system (see Scheme 1), we examined the reaction of dihydrogen (1–4 atm) with **2** in benzene. In initial experiments, after a period of 4–6 h, **2** was consumed as evidenced by ^{31}P NMR spectroscopy and varying amounts of three rhodium–phosphine products were observed; overlapping doublets at δ 32.9 with Rh–P coupling constants of 108 Hz, and a doublet at δ 24.1 with a Rh–P coupling of 110 Hz. Based on the magnitude of the these coupling constants, these are likely Rh(III) species. Upon workup, we were able to obtain crystals of one of these species; the ^{1}H NMR spectrum of the crystalline material, which corresponds to the ^{31}P NMR doublet at δ 32.9, shows a hydride pattern (doublet of triplets) at δ −17.5 and a singlet at δ 2.0; these two peaks integrate to 2H and 1H respectively *versus* the silyl methyl resonances. There is no evidence of coordinated or free cyclooctene and the overall symmetry of this species is C_{2v}. The single-crystal X-ray diffraction study (Fig. 3) revealed its structure (*vide infra*) as the Rh(III)–amine dihydride, Rh[P_2N_2H](H)$_2$ (**3**); the bond lengths and angles match other similar Rh systems, but what is evident is that the N–H unit is localized on one disilylamido unit in the structure, but in solution must be in fast exchange to the other amido unit to generate the higher symmetry observed by ^{1}H NMR spectroscopy (*vide infra*). The geometry about the Rh(III) centre is distorted octahedral; the P1–Rh1–P2, N1–Rh1–H1R and N2–Rh2–H2R bond angles (172.072(15)°, 177(1)° and 176.1(8)° respectively) demonstrate the distortion from idealized octahedral geometry

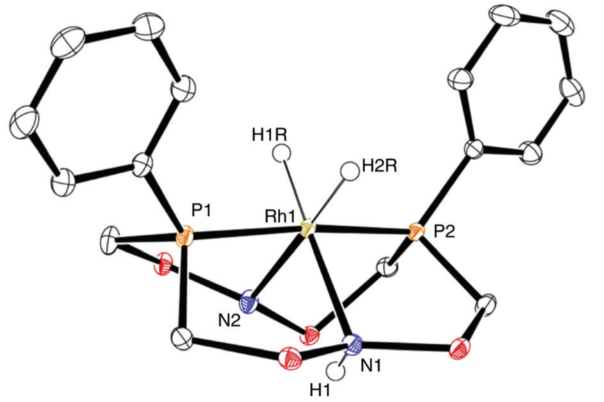

Fig. 3 ORTEP depiction (ellipsoids at 50% probability) of Rh[P_2N_2H](H)$_2$ (**3**). Silyl methyl carbons and all hydrogen atoms except for those bound directly to Rh1 and to N1 are omitted for clarity. Selected bond lengths (Å) and angles (°): Rh1–N1, 2.3305(13); Rh1–N2, 2.2583(13); Rh1–P1, 2.2868(4); Rh1–P2, 2.2670(4); Rh1–H1R, 1.57(3); Rh1–H2R, 1.62(2); N1–H1, 0.74(2); P1–Rh1–P2, 172.072(15); N2–Rh1–H1R, 177(1); N1–Rh1–H2R, 176.1(8).

Reproducibility was initially problematic. While all three products were evident for these experiments, the relative amounts varied considerably. We were able to determine early on that the source of the protonated amido unit in Rh[P_2N_2H](H)$_2$ (**3**) resulted from adventitious water likely from the H_2 source. Careful drying of the dihydrogen resulted in formation of only two lithium–rhodium hydride products: the major product is the dihydride **4** and the minor species formed is the phenyl-hydride **5** (Scheme 4). Both of these Rh(III) products were characterized by single crystal X-ray diffraction (Fig. 4 and 5) and NMR spectroscopy. Additional experiments showed that the phenyl-hydride **5** slowly converts to the dihydride **4** under continued reaction with H_2. When the reaction is conducted in C_6D_6 under H_2, we still observed the two products in the ^{31}P NMR spectrum, which are the dihydride **4** and the deuterio-phenyl-deuteride, ([Rh(C_6D_5)D][P_2N_2]Li)$_2$(dioxane). In the absence of H_2, dissolution of **2** in benzene and slight heating produces the phenyl-hydride selectively.

Monitoring the reaction of ([Rh(COE)][P_2N_2]Li)$_2$(dioxane) (**2**) with dry H_2 by ^{1}H NMR spectroscopy in C_6D_6 shows free cyclooctene in the early stages, but this is eventually converted to cyclooctane. This suggests that the dissociation of cyclooctene is the first step in the hydrogenation of each of the 18-electron rhodium centers in **2**.

As mentioned above, carbon–hydrogen bond activation of benzene to generate phenyl-hydride **5** was confirmed by

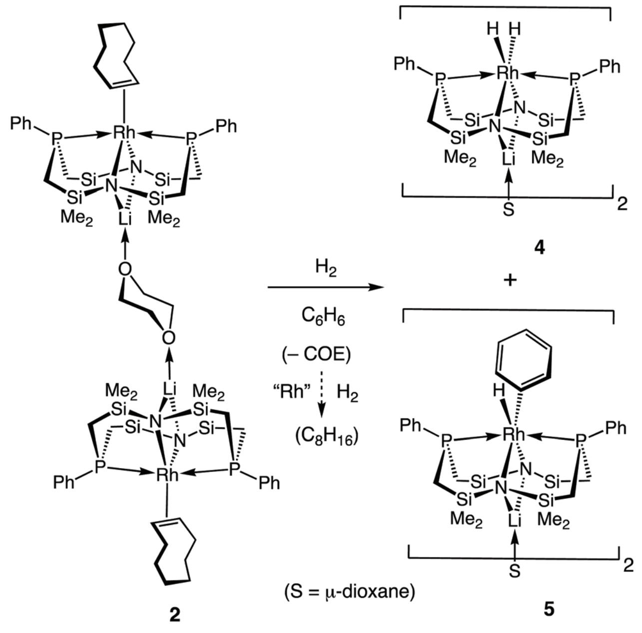

Scheme 4 Reaction of **2** with dry H_2 in C_6H_6.

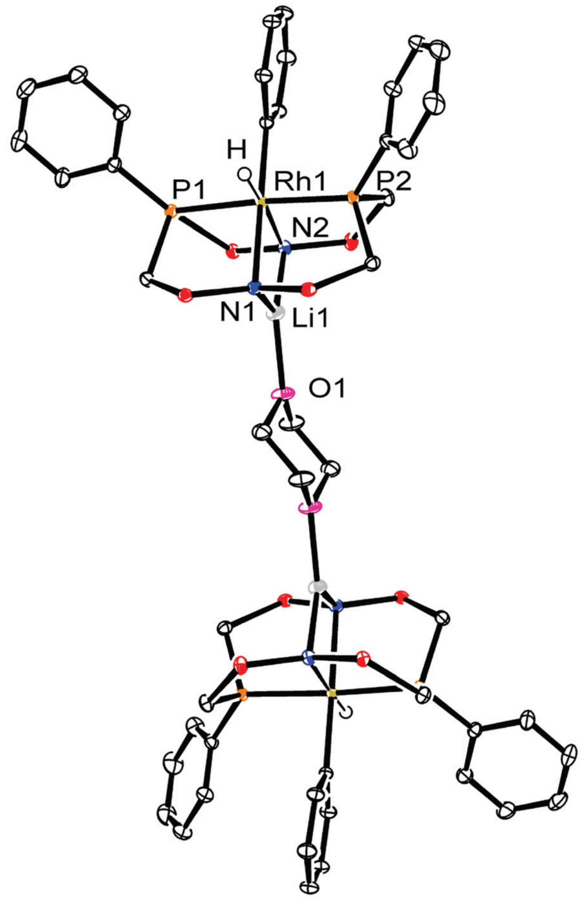

Fig. 4 ORTEP depiction (ellipsoids at 50% probability) of **5**. Silyl methyl carbons and all hydrogen atoms except for those bound directly to Rh are omitted for clarity. Selected bond lengths (Å) and angles (°): Rh1–N1, 2.330(1); Rh1–N2, 2.4144(9); Rh1–P1, 2.2929(4); Rh1–P2, 2.2921(4); Rh1–H1, 1.47(2); N1–Li1, 1.997(2); N2–Li1, 2.052(3); P1–Rh1–P2, 173.27(3); N1–Rh1–H1, 89.1(8); N1–Rh1–N2, 88.86(3).[14]

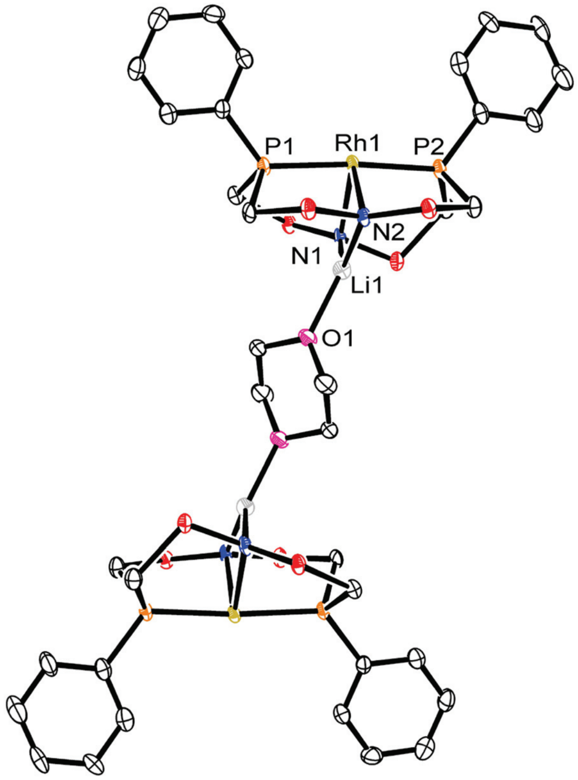

Fig. 5 ORTEP depiction (ellipsoids at 50% probability) of ([Rh(H)$_2$][P$_2$N$_2$]Li)$_2$(dioxane) (**4**). Silyl methyl carbons are omitted for clarity. The hydride atoms could not be located and refined accurately on the density map; however, their presence is confirmed by ^{1}H NMR spectroscopy. The compound crystallized with two molecules in the asymmetric unit; only one molecule is shown but bond metrics for both molecules are listed below. Selected bond lengths (Å) and angles (°): Rh1–N1, 2.338(5)/2.336(6); Rh1–N2, 2.300(6)/2.289(5); Rh1–P1, 2.289(2)/2.281(2); Rh1–P2, 2.275(2)/2.270(2); P1–Rh1–P2, 174.29(6)/–174.99(6); N1–Rh1–N2, 89.7(2)/89.0(2).

heating **2** in neat C_6H_6 in the absence of H_2, which generated good yields of the lithium–rhodium phenyl-hydride species. Other aromatic solvents such as toluene and 1,2-difluorobenzene also underwent C–H activation with mild heating; this will be reported separately.

NMR spectroscopy was crucial in characterizing both the lithium–rhodium-dihydride **5** and the lithium–rhodium–phenyl-hydriide **6**. For **5**, a doublet at *δ* 32.9 in the $^{31}P\{^1H\}$ NMR spectrum with a Rh–P coupling of 107 Hz is observed. In the ^{1}H NMR spectrum, an upfield doublet of triplets resonance at *δ* −16.8, that integrates to 4H (relative to the silyl-methyl signals), is consistent with the presence of two equivalent rhodium hydrides. There are two silyl-methyl singlets at *δ* 0.20 and 0.29, each of which integrates to 24H for the two LiRh[P$_2$N$_2$] fragments; there is also a sharp singlet at *δ* 3.5 that integrates to 8H for the bridging 1,4-dioxane molecule. Overall, the lithium–rhodium-dihydride displays C_{2v} symmetry. The lithium–rhodium–phenyl hydride **6** is less symmetric as there are four silyl-methyl singlets evident in the ^{1}H NMR spectrum, and the methylene (PCH$_2$Si) protons in the macrocyclic backbone generate two sets of multiplets. The two lithium–rhodium P$_2$N$_2$ units are equivalent as are the two Rh–H moieties. The Rh–Ph unit displays slightly upfield multiplets for the aromatic protons as compared to the *P*-phenyl protons of the P$_2$N$_2$ ligand.

The observation of the mononuclear amine-dihydride **3** in the initial reactions with H_2 was investigated further. Addition of a small amount of H_2O to ([Rh(COE)][P$_2$N$_2$]Li)$_2$(dioxane) (**2**) in THF led to reasonable yields of the rhodium(I) amine-cyclooctene complex Rh[P$_2$N$_2$H](COE) (**6**) as shown in Scheme 5. Unlike the lithium–rhodium-cyclooctene complex **2**, the ^{31}P NMR spectrum displays a broad doublet ($^1J_{\text{Rh–P}}$ = 134 Hz), which indicates free rotation of the COE unit, and equivalent phosphorus nuclei on the NMR time scale. Cooling a solution of the rhodium(I) amine-cyclooctene complex **3** in C_7D_8 shows broadening and eventual formation of a similar 8 line pattern (AMX) to **2** indicative of slow rotation of the COE unit, which generates inequivalent phosphines. We attribute this difference in the COE rotational barriers to the subtle steric demands of the splayed *P*-phenyl groups in solution for these complexes.

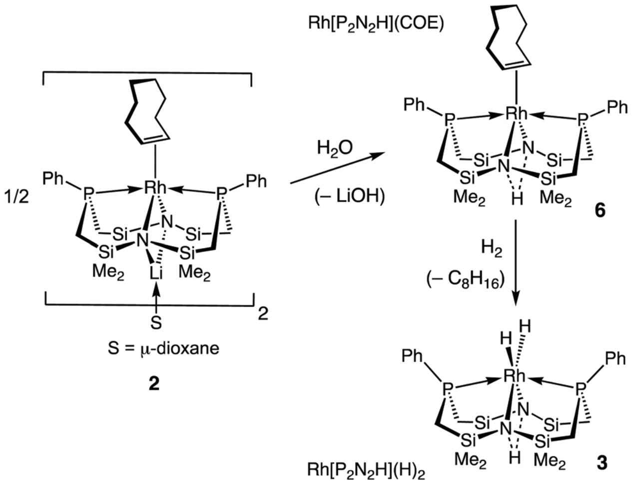

Scheme 5 Protonation of the dilithium–dirhodium-cyclooctene complex **2** to generate the amine–rhodium species, $Rh[P_2N_2H](COE)$, **5** followed by addition of H_2 to produce the amine dihydride $Rh[P_2N_2H](H)_2$ **3**.

As mentioned above, we first observed protonation of the macrocyclic P_2N_2 rhodium–lithium species in the reaction with H_2, presumably due to adventitious H_2O. Reaction of $Rh[P_2N_2H](COE)$ with H_2 leads to the identical rhodium–dihydride-amine **3** observed as a minor side product in the reaction of **2** with H_2 due to the presence of H_2O. The apparent C_{2v} symmetry in solution suggests that the N–H unit is shared or rapidly moves between the two disilyl units as shown in Scheme 5.

The solid-state single crystal X-ray structures of both **3** and **6** (Fig. 3 and 6, respectively) show localized N–H units and in one case, the H–NSi_2 moiety is not coordinated to the rhodium center of **6**; in other words, the former Rh(III) is octahedral and the latter Rh(I) is square planar, in the solid state.

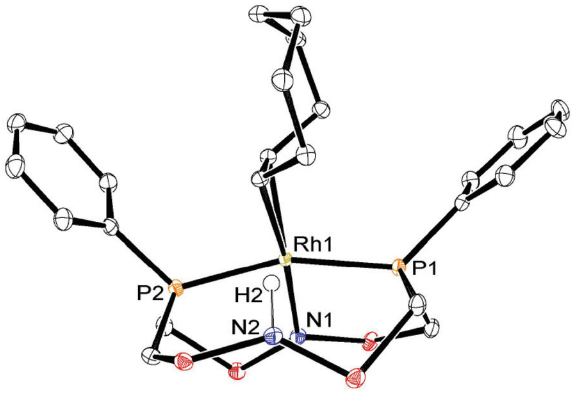

Fig. 6 ORTEP depiction (ellipsoids at 50% probability) of $Rh[P_2N_2H](COE)$ (**6**). Silyl methyl carbons and all hydrogen atoms except the NH are omitted for clarity. The H atom attached to N2 was located on the difference map and refined isotropically. Selected bond lengths (Å) and angles (°): Rh1–N1, 2.117(2); Rh1–P1, 2.3358(7); Rh1–P2, 2.3095(7); P1–Rh1–P2, 157.73(3); N1–Rh1–P1, 87.54(6); N1–Rh1–P2, 84.89(6).

These geometries are different than the lithium congeners, **2** and **4**, which are trigonal bipyramidal and octahedral, respectively, in the solid state. The rhodium–amido bond lengths are comparable to others reported here and elsewhere.[7–9] The Rh–H bond distances are similar to others reported.[14]

We briefly investigated the ability of the protonated Rh(I) system, $Rh[P_2N_2H](COE)$ to activate aromatic C–H bonds akin to the lithium–rhodium cyclooctene analog **2**. Dissolution of $Rh[P_2N_2H](COE)$ in C_6D_6 and heating overnight resulted in loss of the signals due to the starting material and formation of a number of new products, none of which we could identify conclusively. It may well be that the putative Rh(III) amine–phenyl-hydride, $Rh[P_2N_2H](Ph)H$, is inaccessible *via* this route or unstable once formed.

Conclusions

We report the preparation, structure and reactivity of the macrocyclic $[P_2N_2]$ rhodium complexes, $[P_2N_2][Rh(COD)]_2$ (**1**) and $([Rh(COE)][P_2N_2]Li)_2$(dioxane) (**2**) and their reactivity with H_2. Rhodium hydride species were observed upon exposure of both Rh(I) complexes to H_2 gas. In the case of $[P_2N_2][Rh(COD)]_2$, hydride signals were detected in the ^1H NMR spectrum along with consumption of the starting dirhodium starting material; however, no products could be isolated or characterized. In contrast, the more labile cyclooctene precursor, **2** undergoes oxidative addition of H_2 and aromatic C–H bonds when exposed to dihydrogen in aromatic solvents. The reaction with H_2 was initially complicated by the presence of H_2O, which resulted in the isolation of the dihydride-amine, $Rh[P_2N_2H](H)_2$ (**3**), which could be prepared separately by protonation of **2** followed by addition of dihydrogen. In all of the reactions with dihydrogen, coordinated cyclooctene is hydrogenated to cyclooctane, which bodes well for the use of these complexes in catalytic processes.

Experimental

General procedures

All experiments used oven- or flame-dried glassware cooled under vacuum and were performed under an atmosphere of dry, oxygen-free dinitrogen, using standard Schlenk techniques or glovebox (equipped with a −40 °C freezer). Anhydrous hexanes, toluene and THF were purchased from Aldrich, sparged with dinitrogen, passed through towers containing activated alumina and collected over activated molecular sieves. Pentane was distilled from sodium benzophenone ketyl and collected over activated molecular sieves. Hexamethyldisiloxane (HMDSO) was dried over activated molecular sieves and degassed using three freeze–pump–thaw cycles. Benzene-d_6 and toluene-d_8 were dried with sodium benzophenone ketyl, trap-to-trap distilled, and freeze–pump–thaw degassed. ^1H, ^{31}P, ^{29}Si, ^7Li and 2D NMR spectra were recorded on either a Bruker Avance 300 or 400 MHz spectrometer at room temperature unless otherwise noted. The $^{31}P\{^1H\}$ NMR spectra were referenced to external 85% H_3PO_4 at 0.0 ppm. Elemental analyses (EA) were performed using a Thermo Flash 2000 Elemental Analyzer by Mr Derek Smith or Ms. Jenny Lai, at the Department of Chemistry, University of British Columbia. Some microanalysis measurements were performed in open air due to restrictions caused by the COVID-19 pandemic. The compounds synthesized in this paper are highly air- and moisture-sensitive and as a result some of the experimental CHN values differ from the calculated values. X-ray data collection and refinement procedures are described in the ESI.† Unless otherwise noted, reagents were obtained from commercial sources and used as received. H_2 (99.99%), CO and Regen gas (10% H_2, 90% N_2) were purchased from Praxair and passed through activated molecular sieves prior to use.

$[P_2N_2][Rh(COD)]_2$ (1). Solid *syn*-$Li_2[P_2N_2]$(1,4-dioxane) (129 mg, 0.203 mmol) and $[Rh(COD)Cl]_2$ (100 mg, 0.203 mmol) were weighed into the same vial and put in the glovebox freezer for 30 minutes, along with another vial containing 10 mL of toluene. The cold toluene was added to the cold solids and the cloudy orange-yellow mixture was left to stir overnight. The solvent was removed under vacuum and the dark yellow residue was extracted into 4 mL of toluene. The resulting cloudy solution was filtered over Celite. The clear orange-yellow filtrate was condensed to a smaller volume (1–2 mL) and the concentrated solution was stored in the freezer until crystal growth was observed. The solution was decanted and the crystals were dried under vacuum. The yellow crystalline solid was weighed (132 mg, 68% yield) and stored in the freezer. $^1H\{^{31}P\}$ NMR (C_6D_6, 400 MHz): δ 0.3, 0.5, 0.7, 1.1 (s, 6H each, SiCH_3), 1.4–2.0 (m, overlapping signals, approx. 18 H, Si–CH_2–P, COD CH_2), 2.2, 2.3, 2.6, (m, 2 H each, COD CH_2), 3.0, 3.6, 5.3, 5.4 (m, 2H each, COD $HC{=}CH$), 7.0 (t, 2H, *p*-C_6H_5–P), 7.1 (t, 4H, *m*-C_6H_5–P), 7.5 (d, 4H, *o*-C_6H_5–P). $^{31}P\{^1H\}$ NMR (C_6D_6, 161.9 MHz): δ 20.0 (d, J_{RhP} = 143 Hz). $^{13}C\{^1H\}$ NMR (C_6D_6, 100.6 MHz): δ 6.4, 9.5, 9.6, 10.1 (SiCH_3), 18.8, 24.2, 28.3, 34.1 (COD CH_2), 30.5, 31.2, (Si–CH_2–P), 68.2, 71.1, 96.4, 100.9 (COD $HC{=}CH$), 128.2, 128.3, 129.0, 130.7 (C_6H_5–P). Anal. calcd for $C_{40}H_{66}N_2P_2Si_4Rh_2$: C, 50.30; H, 6.97; N, 2.93. Found: C, 49.41; H, 7.12; N, 2.43.

$([Rh(COE)][P_2N_2]Li)_2$(dioxane) (2). A solution of *syn*-$Li_2[P_2N_2]$(1,4-dioxane) (197 mg, 0.310 mmol) in 5 mL of toluene with 0.5 mL of dioxane and a solution of $[Rh(COE)_2Cl]_2$ (111 mg, 0.155 mmol) in 5 mL of toluene was prepared and cooled in the glovebox freezer for 1 h. The $[Rh(COE)_2Cl]_2$ solution was added dropwise to the *syn*-$[P_2N_2]Li_2$(1,4-dioxane) solution while stirring. After the addition was complete, the mixture was immediately put under vacuum to remove the solvent. The remaining solids were extracted into 2 mL of toluene and filtered through a glass filter pad within a pipette, to remove LiCl. The filtrate was evaporated to dryness and the remaining brown residue was triturated with 1 mL of cold hexane. The dark brown solution was decanted and the solids were washed with another 1 mL of cold hexane. The solution was decanted and the yellow-brown solid was dried under vacuum and weighed (199 mg, 81% yield). $^1H\{^{31}P\}$ NMR (C_6D_6, 400 MHz): δ 0.28, 0.36 (s, overlapping, 24 H, SiCH_3), 0.65, 0.72 (s, overlapping, 24 H, SiCH_3), 0.9–1.1 (m, overlapping signals, approx. 12H, COE CH_2, Si–CH_2–P), 1.2, 1.4 (m, overlapping signals, approx. 8H each, COE CH_2, Si–CH_2–P), 1.6, 1.7 (d, 4H each, Si–CH_2–P) 1.8 (m, 4H COE CH_2), 2.0 (br, 4H, COE $HC{=}CH$), 3.5 (s, 8H, $C_4H_8O_2$), 7.0–7.1 (m, approx. 12H, overlapping with residual C_6D_6 proton signal, C_6H_5–P), 7.5 (m, 8H, C_6H_5–P). $^{31}P\{^1H\}$ NMR (C_6D_6, 161.9 MHz): δ 11.5 (dd, J_{RhP} = 123 Hz, J_{PP} = 384 Hz), 23.1 (J_{RhP} = 114 Hz, J_{PP} = 384 Hz). ^7Li NMR (C_6D_6, 155.5 MHz): δ 1.31 (s). $^{13}C\{^1H\}$ NMR (C_6D_6, 100.6 MHz): δ 5.7–6.0 (overlapping signals, not well resolved, SiCH_3), 7.3 (SiCH_3), 26.7, 32.3 (Si–CH_2–P), 26.4, 29.5, 32.6 (COE CH_2), 43.0 (COE $HC{=}CH$), 67.4 ($C_4H_8O_2$), 127.4, 127.6, 131.2, 131.7 (C_6H_5–P). Anal. calcd for $C_{68}H_{120}Li_2N_4O_2P_4Si_8Rh_2$: C, 51.24; H, 7.59; N, 3.51. Found: C, 50.56; H, 7.70; N, 3.46.

$Rh[P_2N_2H](H)_2$ (3). A solution of **2** (44 mg, 0.028 mmol) in 10 mL of toluene was transferred into a thick-walled glass vessel equipped with a Teflon valve and thoroughly degassed *via* 3 freeze–pump–thaw cycles. The vessel was cooled under liquid N_2 and H_2 gas was added. The vessel was sealed and the frozen solution was allowed to warm to RT. The solution was stirred overnight. The H_2 and solvent was removed under vacuum, leaving yellow solid. The solid was extracted into 2 mL hexane and filtered over a glass filter pad within a pipette, removing a light solid. The clear yellow filtrate was evaporated to dryness and the remaining yellow residue was triturated with minimal HMDSO, precipitating a yellow solid. The solution was decanted and the solid was dried under vacuum (26 mg, 74% yield). Crystals suitable for X-ray diffraction were isolated from a concentrated pentane solution stored at −40 °C. ^1H NMR (C_6D_6, 400 MHz): δ −17.5 (dt, 2H, Rh–H, J_{HP} = 14 Hz, J_{HH} = 25 Hz), 0.27, 0.29, (s, overlapping, 24H, SiCH_3), 1.4, 1.6 (dt, 4H each, Si–CH_2–P, J_{HP} = 4 Hz, J_{HH} = 14 Hz), 2.0 (s, 1H, N–H), 7.1 (m, 2H, C_6H_5–P), 7.2 (m, approx. 4H, overlapping with C_6D_6 residual proton, C_6H_5–P), 8.1 (m, 4H, C_6H_5–P). $^{31}P\{^1H\}$ NMR (C_6D_6, 161.9 MHz): δ 32.9 (d, J_{RhP} = 108 Hz). $^{13}C\{^1H\}$ NMR (C_6D_6, 100.6 MHz): δ 3.6, 5.4 (SiCH_3), 28.2 (Si–CH_2–P), 128.3, 129.8, 132.8, 140.9 (C_6H_5–P). Anal. calcd for $C_{24}H_{45}N_2P_2Si_4Rh_1$: C, 45.12; H, 7.10; N, 4.39. Found: C, 43.04; H, 7.12; N, 3.09.

$([Rh(H)_2][P_2N_2]Li)_2$(dioxane) (4). A solution of **2** (63 mg, 0.040 mmol) in 15 mL of C_6H_6 was prepared in the glovebox in a thick-walled glass vessel equipped with a Teflon valve. The solution was degassed *via* one freeze–pump–thaw cycle and then the clear yellow solution was allowed to warm to room temperature. The vacuum line was filled with 1 atm of H_2 gas and the Teflon valve was opened, allowing H_2 gas to flow into the flask. The solution was stirred for 4 days and the color slowly faded to generate a nearly colorless solution. At this point a 0.5 mL sample was removed from the reaction and mixed with 0.5 mL C_6D_6 for an *in situ* NMR analysis. Only one signal existed in the hydride region of the ^1H NMR spectrum and one doublet in the ^{31}P NMR spectrum, both of which correspond to the intended dihydride product **4**. The ^1H NMR spectrum shows that the solution consists primarily of a mixture of **4** and cyclooctane, confirming that the cyclooctene ligand has been fully hydrogenated to cyclooctane. The solvent was removed under vacuum and the resulting solid was redissolved in minimal hexanes (about 5 ml) and allowed to stand in the freezer overnight. The resulting white crystals were isolated by pipetting off the supernatant and were then rinsed with 3 × 1 mL of cold hexanes and dried under vacuum (28 mg, 50% yield). Crystals suitable for X-ray diffraction were isolated from a concentrated hexanes solution stored in the freezer for several days. ^{1}H NMR (C$_6$D$_6$, 400 MHz): δ −16.8 (dt, 4H, Rh–H, J_{HP} = 14 Hz, J_{HRh} = 25 Hz), 0.20 (s, 24H, Si–CH_3), 0.29 (s, 24H, Si–CH_3), 1.49, 1.62 (dt, 8H each, Si–CH_2–P, J_{HP} = 4 Hz, J_{HH} = 14 Hz), 3.52 (s, 8H, C$_4H_8$O$_2$), 7.1–7.2 (m, 12H, overlapping with C$_6$D$_6$ residual proton, C$_6H_5$–P), 8.2 (m, 8H, C$_6H_5$–P). ^{31}P{^{1}H} NMR (C$_6$D$_6$, 161.9 MHz): δ 32.9 (d, J_{PRh} = 107 Hz). ^{13}C{^{1}H} NMR (C$_6$D$_6$, 100.6 MHz) 4.9 (s, SiCH$_3$), 6.1 (t, SiCH$_3$, J = 3 Hz), 30.4 (t, Si–CH$_2$–P, J = 3 Hz), 67.2 (s, C_4H$_8$O$_2$), 129.8 (s, C_6H$_5$–P), 133.0 (t, C_6H$_5$–P, J = 8 Hz), 140.9 (td, C_6H$_5$–P, J_{CP} = 20 Hz, J_{CRh} = 3 Hz). Anal. calcd for $C_{52}H_{96}N_4O_2P_4Si_8\ Rh_2Li_2$: C, 45.34; H, 7.02; N, 4.07. Found: C, 41.56; H, 6.91; N, 3.18.

([Rh(C$_6$H$_5$)H][P$_2$N$_2$]Li)$_2$(dioxane) (4). A solution of **2** (169 mg, 0.106 mmol) in 20 mL of C$_6$H$_6$ was prepared in the glovebox in a thick-walled glass vessel equipped with a Teflon valve. After stirring for 5 days, NMR analysis revealed that the reaction was only 50% complete. The sealed flask was then brought out of the glovebox and immersed in an oil bath set at 90 °C for 2 hours. The flask was then allowed to cool and brought back into the glovebox. The solution was transferred to a vial and the solvent volume was reduced to about 1 mL under vacuum. 4 mL of hexanes was then added to the flask and it was allowed to stand in the freezer overnight. The resulting white crystals were isolated by pipetting off the supernatant and were then rinsed with 2 mL of cold hexanes and dried under vacuum (113 mg, 70% yield). Crystals suitable for X-ray diffraction were isolated from a concentrated C$_6$H$_6$/hexanes solution stored in the freezer for several days. ^{1}H NMR (C$_6$D$_6$, 400 MHz): δ −16.98 (dt, 2H, Rh–H, J_{HP} = 12 Hz, J_{HRh} = 30 Hz), 0.08 (s, 12H, Si–CH_3), 0.23 (s, 12H, Si–CH_3), 0.39 (s, 12H, Si–CH_3), 0.53 (s, 12H, Si–CH_3), 1.25–1.35 ppm (m, 8H, Si–CH_2–P), 1.52, 1.83 (dt, 4H each, Si–CH_2–P, J_{HP} = 5 Hz, J_{HH} = 14 Hz), 3.37 (s, 8H, C$_4H_8$O$_2$), 6.7–6.85 (m, 6H, C$_6H_5$), 7.0–7.1 (m, 12H, C$_6H_5$), 7.5–7.6 (m, 12H, C$_6H_5$). ^{31}P{^{1}H} NMR (C$_6$D$_6$, 161.9 MHz): δ 24.1 (d, J_{PRh} = 110 Hz). ^{13}C{^{1}H} NMR (C$_6$D$_6$, 100.6 MHz): δ 4.7 (s, SiCH$_3$), 5.4 (m, SiCH$_3$), 5.9 (m, SiCH$_3$), 5.4 (s, SiCH$_3$), 26.4 (m, Si–CH$_2$–P), 26.7 (m, Si–CH$_2$–P), 67.3 (s, C_4H$_8$O$_2$), 120.7 (s, C_6H$_5$), 126.1 (s, C_6H$_5$), 129.2 (s, C_6H$_5$), 132.0 (t, C_6H$_5$, J = 7 Hz), 142.9 (m, C_6H$_5$). Anal. calcd for $C_{64}H_{104}N_4O_2P_4Si_8\ Rh_2Li_2$: C, 50.25; H, 6.85; N, 3.66. Found: C, 46.80; H, 6.17; N, 3.11.

Rh[P$_2$N$_2$H](COE). (A solution of **2** (134 mg, 0.0841 mmol) in 15 mL of THF was prepared in the glovebox and then transferred to a Schlenk Line. 10 drops of freshly degassed water were added to the orange solution and it was stirred for 1 hour over which a color change was observed from orange to yellow. The solvent was then removed under reduced pressure and the residue was dried overnight under high vacuum. The crude product was taken up in 20 mL of hexanes and filtered through Celite, rinsing with 10 mL more hexanes. The volume of the hexanes filtrate was reduced to 4 mL and the solution was stored in the freezer overnight. Orange crystals suitable for X-ray crystallography deposited in the vial. A second crop of crystals was obtained by from the supernatant in a similar manner. The orange crystals were combined and dried under vacuum (84 mg, 67% yield). ^{1}H NMR (C$_6$D$_6$, 400 MHz, T = 298 K): δ 0.47 (s, 12H, Si–CH_3), 0.54 (s, 12H, Si–CH_3), 0.82–1.04 (m, 4H, COE CH_2), 1.09–1.24 (m, 8H, COE CH_2, Si–CH_2–P), 1.29–1.38 (m, 2H, COE CH_2), 1.48 (dt, 4H, Si–CH_2–P, J_{HP} = 14, J_{HH} = 5 Hz), 2.09 (broad d, 2H, COE, J = 13 Hz), 2.47 (broad, 2H, COE), 5.60 (broad s, 1H, NH), 6.98–7.03 (m, 2H, C$_6H_5$–P), 7.07–7.10 (m, 4H, C$_6H_5$–P), 7.43–7.47 (m, 4H, C$_6H_5$–P). ^{31}P{^{1}H} NMR (C$_6$D$_6$, 161.9 MHz, T = 298 K): δ 14.5 (d, J_{PRh} = 134 Hz). ^{31}P{^{1}H} NMR (toluene-d$_8$, 161.9 MHz, T = 188 K): δ 24.4 (dd, J_{RhP} = 135 Hz, J_{PP} = 399 Hz), 4.2 (dd, J_{RhP} = 138 Hz, J_{PP} = 398 Hz). ^{13}C{^{1}H} NMR (C$_6$D$_6$, 100.6 MHz, T = 298 K, ±/x refers to up/down/missing in DEPT-135 spectrum): δ 4.7 (t, (+), SiCH$_3$, J = 2 Hz), 5.8 (s, (+), SiCH$_3$), 23.0 (s, (−), CH$_2$), 26.5 (s, (−), CH$_2$), 31.5 (s, (−), CH$_2$), 32.0 (t, (−), CH$_2$, J = 4 Hz), 59.8 (broad, (+), COE HC═CH), 127.9 (t, (+), C_6H$_5$–P, J = 4 Hz), 128.3 (s, (+), C_6H$_5$–P), 130.6 (t, (+), C_6H$_5$–P, J = 6 Hz), 141.4 (t, (x), C_6H$_5$–P, J = 12 Hz). Anal. calcd for $C_{32}H_{57}N_2P_2RhSi_4$: C, 51.45; H, 7.69; N, 3.75. Found: C, 49.19; H, 7.53; N, 3.18.

Rh[P$_2$N$_2$H](H)$_2$ – synthesis from Rh[P$_2$N$_2$H](COE). A solution of Rh[P$_2$N$_2$H](COE) **6** (10 mg, 0.013 mmol) in 1 mL of C$_6$D$_6$ was prepared in the glovebox in a thick-walled glass vessel equipped with a Teflon valve. The solution was degassed *via* one freeze–pump–thaw cycle and then the clear yellow solution was allowed to warm to room temperature. The vacuum line was filled with 1 atm of H$_2$ gas and the Teflon valve was opened, allowing H$_2$ gas to flow into the flask. The solution was stirred for 3 days and was then transferred to a J Young NMR tube. Both ^{1}H and ^{31}P{^{1}H} NMR spectra confirm that the solution consists of a mixture of Rh[P$_2$N$_2$H](H)$_2$ **3** and cyclooctane (singlet at 1.50 ppm in the ^{1}H NMR spectrum).

Conflicts of interest

There are no conflicts to declare.

Acknowledgements

Funding was provided by NSERC of Canada.

References

1 *Modern Rhodium-Catalyzed Organic Reactions*, ed. P. A. Evans, Wiley-VCH Verlag GmbH & Co. KGaA, Weinheim, 2005.

2 (*a*) F. Konrad, J. Lloret Fillol, H. Wadepohl and L. H. Gade, Bis(oxazolinylmethyl)pyrrole Derivatives and Their Coordination as Chiral "Pincer" Ligands to Rhodium, *Inorg. Chem.*, 2009, **48**, 8523–8535; (*b*) Y. Wang, B. Zheng,

Y. Pan, C. Pan, L. He and K.-W. Huang, C-H and H-H bond activation via ligand dearomatization/rearomatization of a PN^3P-rhodium(I) complex, *Dalton Trans.*, 2015, **44**, 15111–15115; (*c*) J. D. Smith, J. R. Logan, L. E. Doyle, R. J. Burford, S. Sugawara, C. Ohnita, Y. Yamamoto, W. E. Piers, D. M. Spasyuk and J. Borau-Garcia, Cationic mono and dicarbonyl pincer complexes of rhodium and iridium to assess the donor properties of $PC_{carbene}P$ ligands, *Dalton Trans.*, 2016, **45**(32), 12669–12679.

3 (*a*) W. Weng, C. Guo, R. Celenligil-Cetin, B. M. Foxman and O. V. Ozerov, Skeletal change in the PNP pincer ligand leads to a highly regioselective alkyne dimerization catalyst, *Chem. Commun.*, 2006, 197–199; (*b*) C. J. Pell and O. V. Ozerov, A Series of Pincer-Ligated Rhodium Complexes as Catalysts for the Dimerization of Terminal Alkynes, *ACS Catal.*, 2014, **4**, 3470–3480.

4 D. Bezier, C. Guan, K. Krogh-Jespersen, A. S. Goldman and M. Brookhart, Experimental and computational study of alkane dehydrogenation catalyzed by a carbazolide-based rhodium PNP pincer complex, *Chem. Sci.*, 2016, **7**, 2579–2586.

5 L. Schwartsburd, M. A. Iron, L. Konstantinovski, E. Ben-Ari and D. Milstein, A Dearomatized Anionic PNP Pincer Rhodium Complex: C–H and H–H Bond Activation by Metal–Ligand Cooperation and Inhibition by Dinitrogen, *Organometallics*, 2011, **30**, 2721–2729.

6 (*a*) A. Anaby, M. Feller, Y. Ben-David, G. Leitus, Y. Diskin-Posner, L. J. W. Shimon and D. Milstein, Bottom-Up Construction of a CO_2-Based Cycle for the Photocarbonylation of Benzene, Promoted by a Rhodium(I) Pincer Complex, *J. Am. Chem. Soc.*, 2016, **138**, 9941–9950; (*b*) R. H. Lam, D. B. Walker, M. H. Tucker, M. R. D. Gatus, M. Bhadbhade and B. A. Messerle, Intermolecular Hydroalkoxylation of Terminal Alkynes Catalyzed by a Dipyrrinato Rhodium(I) Complex with Unusual Selectivity, *Organometallics*, 2015, **34**, 4312–4317.

7 (*a*) M. D. Fryzuk, New binuclear bis(diphenylphosphino) methane complexes of rhodium(I) incorporating 2-methylallyl ligands, *Inorg. Chim. Acta*, 1981, **54**, L265–L266; (*b*) M. D. Fryzuk, Coordinatively unsaturated clusters of rhodium incorporating chelating bidentate ligands. Synthesis of $[\{(CH_3O)_2PC\ H_2CH_2P(OCH_3)_2\}RhH]_4$ and $[\{(i\text{-}C_3H_7O)_2PC\ H_2CH_2P(O\text{-}i\text{-}C_3H_7)_2\}RhH]_2$, *Organometallics*, 1982, **1**, 408–409; (*c*) M. D. Fryzuk and P. A. MacNeil, Amides of rhodium and iridium stabilized as hybrid multidentate ligands, *Organometallics*, 1983, **2**, 355–356; (*d*) H. Jong, B. O. Patrick and M. D. Fryzuk, Amine-tethered N-heterocyclic carbene complexes of rhodium(I), *Can. J. Chem.*, 2008, **86**, 803–810; (*e*) B. K. Shaw, B. O. Patrick and M. D. Fryzuk, Thermal Rearrangement via P–C Bond Cleavage of a Tridentate Diphosphine–N-Heterocyclic Carbene Ligand System Coordinated to Rhodium, *Organometallics*, 2012, **31**(3), 783–786; (*f*) T. C. Wambach, *Cooperative Ligand Design for Late Transition Metal Coordination Compounds*, University of British Columbia, Vancouver, 2015.

8 (*a*) M. D. Fryzuk, P. A. MacNeil and S. J. Rettig, Rhodium and iridium amides, *Organometallics*, 1986, **5**, 2469–2476; (*b*) M. D. Fryzuk, P. A. MacNeil and N. T. McManus, Carbon-hydrogen bond activation by rhodium and iridium amides: strategy vs. serendipity, *Organometallics*, 1987, **6**, 882–884; (*c*) M. D. Fryzuk, P. A. MacNeil and S. J. Rettig, Stereoselective formation of rhodium and iridium hydrides via intramolecular hydrogen bonding, *J. Am. Chem. Soc.*, 1987, **109**, 2803–2812.

9 (*a*) O. V. Ozerov, C. Guo, V. A. Papkov and B. M. Foxman, Facile Oxidative Addition of N-C and N-H BOnds to Monovalent Rhodium and Iridium, *J. Am. Chem. Soc.*, 2004, **126**, 4792–4793; (*b*) S. Gatard, C. Guo, B. M. Foxman and O. V. Ozerov, Thioether, Dinitrogen, and Olefin Complexes of (PNP)Rh: Kinetics and Thermodynamics of Exchange and Oxidative Addition Reactions, *Organometallics*, 2007, **26**, 6066–6075; (*c*) M. Puri, S. Gatard, D. A. Smith and O. V. Ozerov, Competition Studies of Oxidative Addition of Aryl Halides to the (PNP)Rh Fragment, *Organometallics*, 2011, **30**, 2472–2482; (*d*) D. M. Gerard van Koten, *Organometallic Pincer Chemistry*, Springer Berlin Heidelberg, 2013, vol. 40; (*e*) J. R. Khusnutdinova and D. Milstein, Metal Ligand Cooperation, *Angew. Chem., Int. Ed.*, 2015, **54**, 12236–12273.

10 (*a*) R. J. Burford, A. Yeo and M. D. Fryzuk, Dinitrogen activation by group 4 and group 5 metal complexes supported by phosphine-amido containing ligand manifolds, *Coord. Chem. Rev.*, 2017, **334**, 84–99; (*b*) M. D. Fryzuk, The 1992 Alcan Award Lecture Excursions around the periodic table: ligand design in inorganic chemistry, *Can. J. Chem.*, 1992, **70**, 2839–2845.

11 G. H. Imler, M. J. Zdilla and B. B. Waland, Equilibrium Thermodynamics to Form Rhodium Formyl Compl from Reactions of CO and H_2, *J. Am. Chem. Soc.*, 2014, **136**, 5856–5859.

12 D. W. Meek and T. J. Mazanac, Determination of structural and dynamic aspects of organometallic and coordination chemistry by phosphorus-31 NMR spectroscopy, *Acc. Chem. Res.*, 1981, **14**, 266–274.

13 V. Vasilenko, T. Roth, C. K. Blasius, S. N. Intorp, H. Wadepohl and L. H. Gade, A modular approach to neutral P,N-ligands: synthesis and coordination chemistry, *Beilstein J. Org. Chem.*, 2016, **12**, 846–853.

14 (*a*) A. M. Lilio, M. H. Reineke, C. E. Moore, A. L. Rheingold, M. K. Takase and C. P. Kubiak, Incorporation of Pendant Bases into $Rh(diphosphine)_2$ Complexes: Synthesis, Thermodynamic Studies, And Catalytic CO_2 Hydrogenation Activity of $[Rh(P_2N_2)_2]^+$ Complexes, *J. Am. Chem. Soc.*, 2015, **137**, 8251–8260; (*b*) Y. Hu, L. Li, A. P. Shaw, J. R. Norton, W. Sattler and Y. Rong, Synthesis, Electrochemistry, and Reactivity of New Iridium(III) and Rhodium(III) Hydrides, *Organometallics*, 2012, **31**, 5058–5064.